

# Motion Field Regularization for Sliding Objects Using Global Linear Optimization

Gustaf Johansson, Mats Andersson and Hans Knutsson

*Department of Biomedical Engineering, Linköping University, Linköping, Sweden*  
*Centre of Medical Image Science and Visualization, Linköping University, Linköping, Sweden*

**Keywords:** Image Registration, Missing Data, Medical Image Processing, Global Linear Optimization.

**Abstract:** In image registration it is often necessary to employ regularization in one form or another to be able to find a plausible displacement field. In medical applications, it is useful to define different constraints for different areas of the data. For instance to measure if organs have moved as expected after a finished treatment. One common problem is how to find plausible motion vectors far away from known motion. This paper introduces a new method to build and solve a Global Linear Optimizations (GLO) problem with a novel set of terms which enable specification of border areas to allow a sliding motion. The GLO approach is important especially because it allows simultaneous incorporation of several different constraints using information from medical atlases such as localization and properties of organs. The power and validity of the method is demonstrated using two simple, but relevant 2D test images. Conceptual comparisons with previous methods are also made to highlight the contributions made in this paper. The discussion explains important future work and experiments as well as exciting future improvements to the GLO framework.

## 1 INTRODUCTION

Medical imaging is progressing fast and plays an increasingly important role in both medical diagnosis and patient treatment. Image registration is one sub-field where the objective is to find a plausible mapping between two data sets. This could be to find a motion between two frames in a time sequence or mapping how different organs and tissues have changed or moved after a surgery or treatment. Many natural motions of tissues and organs in the human body are subject to different constraints such as varying degree of sliding and friction, rigid body motion and incompressibility. If methods and treatments in the medical sciences are able to create better models which take into consideration the physical properties of organs, this can lead to more correct diagnosis and better treatments, ultimately improving the health of the patients. Therefore it is important to find good methods to incorporate medical atlas information in the data processing. Regularization of the displacement fields is necessary for most image registration algorithms to get a plausible displacement field. Regularization means correcting noisy estimates and filling in uncertain or missing data with help of parts of the images where motion is more certain. From physics,

various decompositions of vector fields have been investigated for a very long time. Some such decompositions can be used for regularization and are explained in (Ruan et al., 2009). Solenoidal and irrotational decompositions are for instance relevant when putting constraints such as rotational motion and incompressibility of organ interiors. When it comes to find methods for regularization to allow sliding motion of organs the work done in (Pace et al., 2011) are relevant. There a normal vector  $\hat{n}$  with a corresponding proximity or certainty weight  $w \in [0, 1]$  help steer the regularization. Then an anisotropic diffusion is built based on models from physics to which a numerical solution can be found by an iterative algorithm. A previous global regularization (Johansson et al., 2012) introduced the Global Linear Optimization framework for adaptive regularization. In that work, the motion from the initial registration was considered to be more certain in the orientations of a local structure tensor  $\mathbf{T}$ . The method presented in this paper is inspired by all the previously mentioned papers and uses the powerful GLO framework which is able to put constraints on both above types of motion for different areas of the data-set. With those capabilities in mind, the focus in this paper is on finding GLO constraints to allow the sliding motion of objects.

## 2 ALGORITHM DESCRIPTION

### Structural and Tangent Spaces

We denote the tensor which stores information about the local structure of a frictionless surface  $\mathbf{T}$ . Normalization with respect to its largest eigenvalue  $\lambda_1$  is denoted with a hat:

$$\hat{\mathbf{T}} = \frac{\mathbf{T}}{\lambda_1} : \lambda_1 \geq \dots \geq \lambda_N \geq 0 \quad (1)$$

Then, we define the complementary tensor:

$$\mathbf{P} = \mathbf{I} - \hat{\mathbf{T}} \quad (2)$$

This is a tensor which is large in any orientation which  $\mathbf{T}$  isn't. So in the neighbourhood of a surface,  $\mathbf{T}$  has at least one large eigenvalue, and  $\mathbf{P}$  has at least one small eigenvalue, with

$$\lambda_P = 1 - \lambda_{\hat{\mathbf{T}}} \in [0, 1] \quad (3)$$

for each such pair of eigenvalues<sup>1</sup>. Far from any frictionless surface,  $\mathbf{P}$  will be the identity tensor, but close to it will represent the local *tangent space* of the surface.

### Oriental Decompliation

A vector field  $\mathbf{d}$ , in the neighbourhood of a tensor field, we can decompose into normal and tangential components. By construction this decomposition makes sure we don't miss any part of the  $\mathbf{d}$  field:

$$(\mathbf{P} + \hat{\mathbf{T}})\mathbf{d} = \mathbf{I}\mathbf{d} = \mathbf{d} \quad (4)$$

We can now decompose our signal into the normal and tangential components:

$$\mathbf{d}_n = \hat{\mathbf{T}}\mathbf{d} ; \quad \mathbf{d}_t = \mathbf{P}\mathbf{d} \quad (5)$$

We now have the basic building blocks required for our application.

### Convention and Notation

First of all, our vector fields are stored as vectorized scalar images.

$$\mathbf{d} = [\mathbf{d}_1^T, \dots, \mathbf{d}_k^T, \dots, \mathbf{d}_N^T]^T \quad (6)$$

Where  $\mathbf{d}_k$  is a column vector storing the values of the scalar component for dimension  $k$ .

<sup>1</sup>By Brauer's theorem (Horn and Johnson, 1990) together with  $\lambda(\mathbf{T}) \in \mathbb{R}^+$  eigenvalues, the eigensystems of  $\mathbf{T}$  and  $\mathbf{P}$  will coincide.

Expression	Explanation
$\mathbf{d}$	Initial displacement.
$\mathbf{v}$	Additive correction to $\mathbf{d}$ .
$\mathbf{I}_n$	The $n \times n$ identity.
$\otimes$	Kronecker product.
$\frac{\partial(\cdot)}{\partial k}$	Derivative wrt. dim. $k$ .
$\nabla_s = [\frac{\partial(\cdot)}{\partial 1}, \dots, \frac{\partial(\cdot)}{\partial N}]^T$	Scalar gradient.
$\nabla = (\mathbf{I}_N \otimes \nabla_s)$	Vector gradient.

Figure 1: Table for explaining symbols and notation.

### The Tangent Space

We want the vector field to be as smooth as possible along the tangent space. The tangential change of the gradient in the tangential orientation is given by:

$$(\mathbf{I}_N \otimes \mathbf{P})\nabla\mathbf{P} \quad (7)$$

$\mathbf{P}$  first picks out tangential components of the vector field. Then the gradient calculates all spatial partial differentials, the "smoothness" of the tangential components. Finally we only want to punish the parts of those gradients which are in the tangential directions, so we have a final multiplication on each scalar gradient by  $\mathbf{P}$  from the left. Since we want to disallow irregularities in the tangent orientations on the *result*, this constraint should work on the resulting field  $(\mathbf{v} + \mathbf{d})$ .

### The Normal Costs

Now we investigate the costs in the orientation normal to the surface:  $\nabla\mathbf{T}$ , we want to remove any irregularities of the normal component. But this time, we want to do that on the *changes* of the field. Therefore this constraint should punish the additional field  $(\mathbf{v})$  from being too large.

### Filling Out The Spaces

For the gradients above, we choose to use the  $2 \times 2$  partial differential filters below. We then add the checkerboard filter  $\mathbf{H}$  to cause a cost for  $(\mathbf{v} + \mathbf{d})$ , not wanting any such high frequency components in our results. Also the mean value box filter  $\mathbf{L}$  is used, punishing the results of low pass components  $(\mathbf{v} + \mathbf{d})$ . These terms are present for stability - to ensure that the equation system is positive definite. The discrete

filters used in the 2D experiments are as following:

$$\mathbf{D}_x = \begin{bmatrix} 1 & -1 \\ 1 & -1 \end{bmatrix} \quad \mathbf{D}_y = \begin{bmatrix} 1 & 1 \\ -1 & -1 \end{bmatrix} \quad (8)$$

$$\mathbf{L} = \begin{bmatrix} 1 & 1 \\ 1 & 1 \end{bmatrix} \quad \mathbf{H} = \begin{bmatrix} 1 & -1 \\ -1 & 1 \end{bmatrix}$$

### Translating Motion of Objects

Here, we introduce a new condition. For the objects in the experiment, we add a matrix  $\mathbf{S}$  which consists of two rows per object and  $\mathbf{d}_L$ , a vector with two indices per object. The rows of the  $\mathbf{S}$  matrix are mean value filters over all the data points where the object currently resides. The cost term  $\|\mathbf{S}(\mathbf{v} + \mathbf{d}) - \mathbf{d}_L\|_F^2$  then means that the mean value of the resulting vectors for the objects should be close to the prescribed vector  $\mathbf{d}_L$ , this way we can see if the vector field imposed will propagate to an acceptable solution at the friction-free borders. Also in one last experiment, we add the entire interior of the large circle to be one big object and force it to not be able to translate. We leave the solution found open for interpretation.

### Constructing the GLO

$$O(\mathbf{v}) = \|(\mathbf{I}_N \otimes \mathbf{P}) \nabla \mathbf{P}(\mathbf{v} + \mathbf{d})\|_F^2 + \|\nabla \mathbf{T}(\mathbf{v})\|_F^2 + \|(\mathbf{I}_N \otimes \mathbf{L})(\mathbf{v} + \mathbf{d})\|_F^2 + \|(\mathbf{I}_N \otimes \mathbf{H})(\mathbf{v} + \mathbf{d})\|_F^2 + \|\mathbf{S}(\mathbf{v} + \mathbf{d}) - \mathbf{d}_L\|_F^2 \quad (9)$$

Since all the operators in the expressions are linear with respect to  $\mathbf{v}$ , we can find large (sparse) matrices for each term and solve this as a large linear problem. Details of how to solve such a system is in the paper (Johansson et al., 2012). The last two terms are regularizing terms for stability. There is a theoretical foundation for this construction, but it is outside the scope of this work.

### Test Images and Initial Conditions

We have two test images with two test cases each:

1. Test image with a flat border and known movements along the border on each side, but missing data far from the border.
2. Test image with a flat border and unknown movements along the border on each side, but known translative motion of two objects, far from the borders.
3. Test image with a circular border and known translation of two objects, one inside and one outside.

4. Test image with a circular border and known translation of two objects, both inside.
5. Test image with a circular border and known translation of two objects, both inside AND interior of organ is not allowed to translate.

### Practical Considerations

The matrices representing the translational constraint have a number of non-zero values which are proportionate to the area of the object. The matrix expression  $\mathbf{S}^T \mathbf{S}$  then square the number of pixels in the objects. So we really want to not have to calculate and/or store this matrix if we have large objects. Fortunately if we use a conjugate gradient solver, we are able to solve this iteratively without even having to add up and store the left hand side of the equations system.

### Illustrating the Local Metric

Every pixel will exist in four such equations for each filter, so the local metric will have the shape as follows:

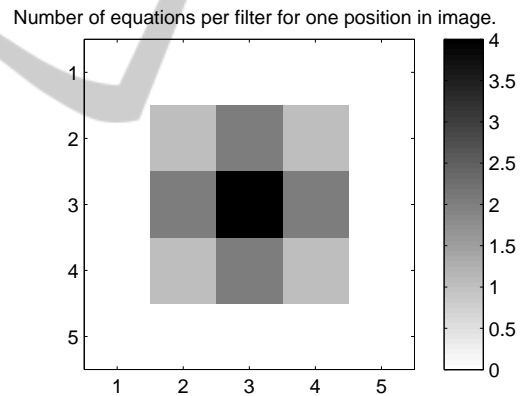


Figure 2: As we can see only pixels within a 8-connectivity are included in the equation system. So our equation system is very sparse and has a *very* localized metric!

### Implementation

The method was implemented in the Matlab programming language. The tensor fields were generated automatically from the test images, so there was no risk for measurement noise - something which could be an issue in a practical use case.

### Conjugate Gradient Solver

A Conjugate Gradient solver was implemented which was very useful for the experiment when the constraint that the large circular organ should not shift

mass centre. Without it calculation times were about 200-300 seconds for the worst cases. Probably most of this time was because  $S^T S$  needed to be specifically calculated and stored. This involves an outer product of the mean value of the interior of the large organ by itself - clearly not a very sparse matrix any longer. Processing times of 10-20 seconds were common when using the Conjugate Gradients solver for the same case. And then not much effort was put into trying to make it any extra efficient. For the experiments without the large organ center-of-mass constraint processing times of 2-3 seconds were common.

### 3 EXPERIMENTS AND RESULTS

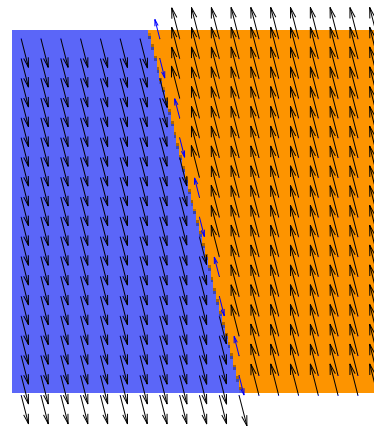


Figure 6: Results for the planar surface experiment with no objects, but known motion close to the border.

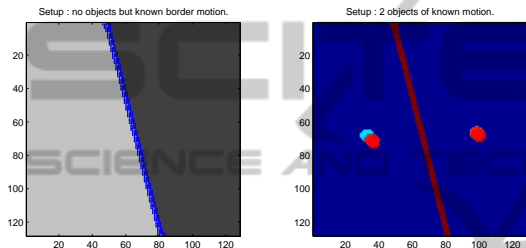


Figure 3: The setup for the planar surface experiments.

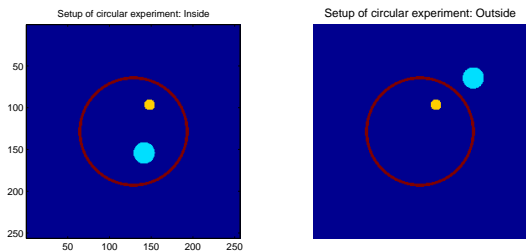


Figure 4: The setup for the circular surface experiments.

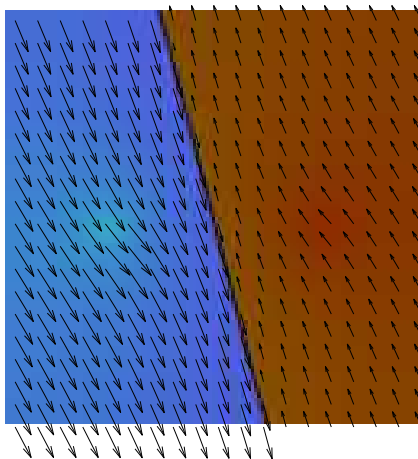


Figure 5: Results for the planar surface experiment with objects.

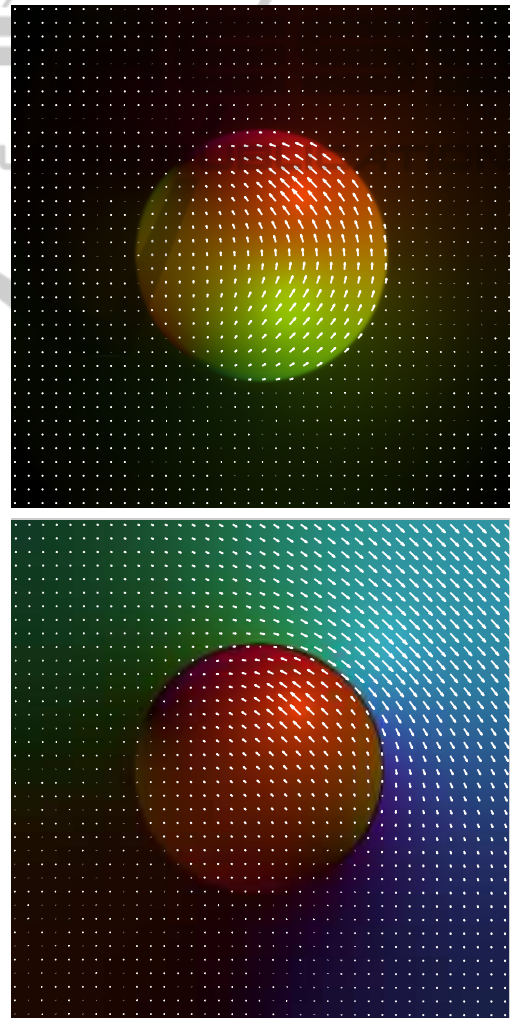


Figure 7: Results for the circular surface experiments. A color image with overlaid quiver shows the resulting vector field.

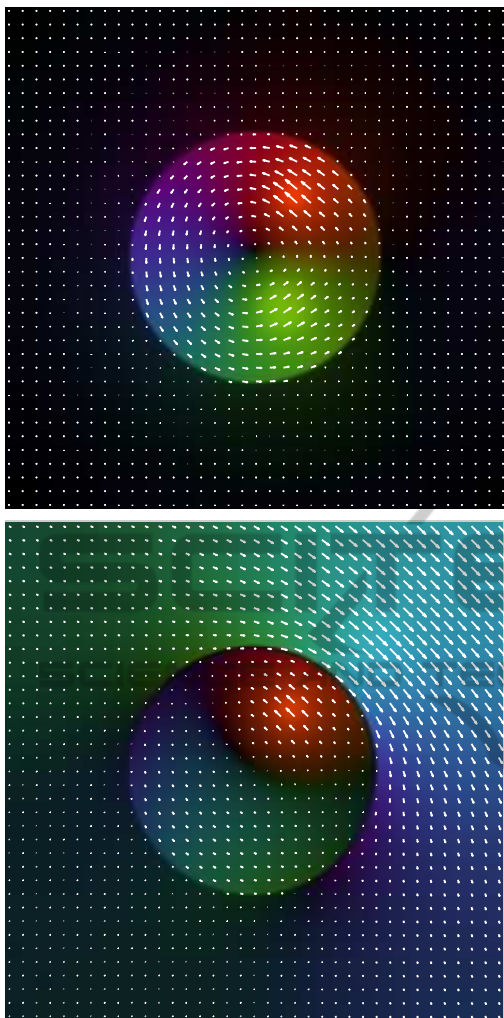


Figure 8: Results for the fixed inner circle.

## 4 CONCLUSIONS

We have demonstrated a method to perform regularization which allows for areas without friction in the regularized field. The method has been demonstrated on six relevant test-cases in 2 dimensions. The methods are shown to work well even if the vast majority of the data is missing. We also demonstrate that the GLO framework used is very powerful and allows for several more simultaneous constraints on different subsets of the data. One of which is known translational motion ( known center-of-mass ), which is incorporated into two of the test cases. This information of how to adapt the processing could be incorporated from for instance medical atlases with a segmentation done beforehand.

The work is inspired by the method used in (Pace

et al., 2011), but our method uses a tensor instead of a vector for the orientations normal to the sliding surface, which allows to treat more complex neighbourhoods - something that would be especially useful for 3D processing. Also the framework in which our method was implemented allows to combine with many other models and behaviours for the data processing - including non-local constraints such as the mass-center constraint demonstrated, which is an especially good property when considering biomedical image processing, where it would be beneficial to simultaneously consider many different physiological constraints in order to increase the chance of a correct diagnosis or a successful medical treatment.

## 5 DISCUSSION

On coarse scales in 3D - for instance cylinders, tubular structures and edges of cuboids,  $\text{rank}(\mathbf{T}) = 2$  and therefore  $\text{rank}(\mathbf{P}) = 1$ . This is not possible if finding an  $\hat{\mathbf{n}}$  to the closest boundary and computing  $\mathbf{P} = (\mathbf{I} - w\hat{\mathbf{n}}\hat{\mathbf{n}}^T)$  as in (Pace et al., 2011).

Despite the conceptual advantages compared to previously mentioned method, important future work remains to be done for the proposed method:

1. Tests where noise is present in  $\mathbf{d}$ .
2. Test cases where noise is present in  $\mathbf{T}$ .
3. Testing for real clinical data.
4. Implementation in 3 dimensions.

Other important future work includes demonstrating combining the proposed method with simultaneously performing the regularization done in (Johansson et al., 2012) and to implement and incorporate GLO functionality similar to that which is described in (Ruan et al., 2009). If all of those types of regularization could be combined it would hopefully give a very powerful platform for global regularization in medical image registration. Very recently, while this work was being done, two new registration algorithms which handle sliding of objects were published (Lianghao et al., 2014) and (Berendsen et al., 2014). It is difficult for our proposed regularization method to directly compare to theirs partly because of conceptual differences but mostly because they present entire registration methods and not only methods for regularization of missing or uncertain data.

## ACKNOWLEDGEMENTS

We would like to thank the Swedish Research Council, grant 2011-5176 for project: *Dynamic Context*

*Atlases for Image Denoising and Patient Safety* and CADICS - a Linnaeus Research Environment for funding this research.

## REFERENCES

- Berendsen, F. F., Kotte, A. N. T. J., Viergever, M. A., and Pluim, J. P. W. (2014). Registration of organs with sliding interfaces and changing topologies. In *Proc. SPIE 9034, Medical Imaging 2014: Image Processing*, 90340E.
- Horn, R. A. and Johnson, C. R. (1990). *Matrix Analysis*. Cambridge University Press.
- Johansson, G., Forsberg, D., and Knutsson, H. (2012). Globally optimal displacement fields using local tensor metric. In *Proceedings of the International Conference on Image Processing (ICIP)*.
- Lianghao, H., Hawkes, D., and Barrat, D. (2014). A hybrid biomechanical model-based image registration method for sliding objects. In *Proc. SPIE 9034, Medical Imaging 2014: Image Processing*, 90340G.
- Pace, D., Enquobahrie, A., Yang, H., Aylward, S., and Nithammer, M. (2011). Deformable image registration of sliding organs using anisotropic diffusive regularization. In *Biomedical Imaging: From Nano to Macro, 2011 IEEE International Symposium on*, pages 407–413.
- Ruan, D., Esedoglu, S., and Fessler, J. (2009). Discriminative sliding preserving regularization in medical image registration. In *Biomedical Imaging: From Nano to Macro, 2009. ISBI '09. IEEE International Symposium on*, pages 430–433.

## APPENDIX

For clarification we here write down explicit expressions for some of the terms in the GLO. Assume matrices have elements denoted as in:

$$\mathbf{A} = \begin{pmatrix} a_{11} & a_{12} & \cdots & a_{1N} \\ a_{21} & a_{22} & \cdots & a_{2N} \\ \vdots & \vdots & \ddots & \vdots \\ a_{M1} & a_{M2} & \cdots & a_{MN} \end{pmatrix} \quad (\text{A.10})$$

A Kronecker product  $\otimes$  between two matrices  $\mathbf{A}$  and  $\mathbf{B}$  is:

$$\mathbf{A} \otimes \mathbf{B} = \begin{pmatrix} a_{11}\mathbf{B} & a_{12}\mathbf{B} & \cdots & a_{1N}\mathbf{B} \\ a_{21}\mathbf{B} & a_{22}\mathbf{B} & \cdots & a_{2N}\mathbf{B} \\ \vdots & \vdots & \ddots & \vdots \\ a_{M1}\mathbf{B} & a_{M2}\mathbf{B} & \cdots & a_{MN}\mathbf{B} \end{pmatrix} \quad (\text{A.11})$$

So in our case for 2D,  $\mathbf{I}_2$  and the  $\mathbf{P}$  tensor are:

$$\mathbf{I}_2 = \begin{pmatrix} 1 & 0 \\ 0 & 1 \end{pmatrix} \quad \mathbf{P} = \begin{pmatrix} \mathbf{P}_{11} & \mathbf{P}_{12} \\ \mathbf{P}_{12} & \mathbf{P}_{22} \end{pmatrix} \quad (\text{A.12})$$

And then the kronecker product to work on each of the spatial gradient becomes:

$$(\mathbf{I}_2 \otimes \mathbf{P}) = \begin{pmatrix} \mathbf{P}_{11} & \mathbf{P}_{12} & \mathbf{0} & \mathbf{0} \\ \mathbf{P}_{12} & \mathbf{P}_{22} & \mathbf{0} & \mathbf{0} \\ \mathbf{0} & \mathbf{0} & \mathbf{P}_{11} & \mathbf{P}_{12} \\ \mathbf{0} & \mathbf{0} & \mathbf{P}_{12} & \mathbf{P}_{22} \end{pmatrix} \quad (\text{A.13})$$

For  $\nabla = \mathbf{I}_2 \otimes \nabla_s$ , we get for 2D:

$$\begin{pmatrix} 1 & 0 \\ 0 & 1 \end{pmatrix} \otimes \begin{pmatrix} \frac{\partial}{\partial x} \\ \frac{\partial}{\partial y} \end{pmatrix} = \begin{pmatrix} \frac{\partial}{\partial x} & 0 \\ \frac{\partial}{\partial y} & 0 \\ 0 & \frac{\partial}{\partial x} \\ 0 & \frac{\partial}{\partial y} \end{pmatrix} \quad (\text{A.14})$$